



Stable isotopes in cave ice suggest summer temperatures in East-Central Europe are linked to AMO variability

Carmen-Andreea Bădăluță^{1,2,3}, Aurel Perșoiu^{1,4}, Monica Ionita⁵, Natalia Piotrowska⁶

¹Stable Isotope Laboratory, Ștefan cel Mare University, Suceava, 720229, Romania

5 ²Department of Geography, Ștefan cel Mare University, Suceava, 720229, Romania

³Institute for Geological and Geochemical Research, Research Centre for Astronomy and Earth Sciences MTA, Budapest, 1112, Hungary

⁴Emil Racoviță Institute of Speleology, Romanian Academy, Cluj Napoca, 400006, Romania

⁵Alfred Wegener Institute, Helmholtz Center for Polar and Marine Research, Bremerhaven, 27515, Germany

10 ⁶Institute of Physics, Silesian University of Technology, Gliwice, 44-100, Poland

Correspondence to: Carmen-A. Bădăluță (carmen.badaluta@usm.ro), Aurel Perșoiu (aurel.persoiu@gmail.com)

Abstract. The climate of East-Central Europe (ECE) is the result of the combination of influences originating in the wider North Atlantic realm, the Mediterranean Sea and Western Asia/Siberia. Climate models suggest that these competing influences will result in difficult to predict responses to the ongoing climatic changes, thus making mitigation and adaptation strategies challenging to devise and implement. Previous studies have shown that the complex interplay between the large-scale atmospheric patterns across the region result in strongly dissimilar summer and winter conditions on time scales ranging from decades to millennia. To put these into a wider context, long term climate reconstructions are required, but, largely due to historical reasons, these are lacking in ECE. We address these issues by presenting a high resolution, precisely dated record of summer temperature variations during the last millennium in ECE, based on stable isotopic analysis performed on a 4.84 m long ice core extracted from Focul Viu Ice Cave (Western Carpathians, Romania). The data shows little summer temperature differences between the Medieval Warm Period and the Little Ice Age on centennial scales, but with well-expressed minima and maxima occurred synchronously with periods of low and high solar activity. Further, summer temperatures fluctuated with a periodicity similar to that of the Atlantic Multidecadal Oscillation, suggesting that solar variability-induced climatic changes were transferred locally by atmospheric processes. Contrary to summer temperatures, winter ones show stronger contrast between the MWP and LIA, thus suggesting that the later were likely an expression of winter climatic conditions.

15
20
25

1 Introduction

The rapid global warming (IPCC, 2018) and the ensuing suite of climatic changes that it triggers (Coumou and Rahmstorf, 2012) demands a clear understanding of the mechanisms behind them in order to be able to disentangle natural and anthropogenic processes (Haustein et al., 2017; IPCC, 2018). Especially important are high-resolution reconstructions of the past variability of specific climatic variables – seasonal air temperatures and precipitation amounts being the most important - that allow for direct comparisons with the dynamics of natural forcing and further deciphering the mechanisms of past and present climate dynamics. The last 1000 years are particularly significant, as the European climate changed from, generally, warm to cold (the Medieval Warm Period-Little Ice Age transition, Jones et al., 2009) and back to warm (the present-day warming, Neukom et al., 2019) and these transitions allow for testing the links between forcing and climatic response. While several global (Jones and Mann, 2004; Mann et al, 2009) and hemispheric (Moberg et al, 2005; Neukom et al., 2019; PAGES 2k Consortium, 2019; Ljungqvist et al., 2019) climatic reconstructions have been published, these made no seasonal differentiation – a task that became recently increasingly necessary to constrain the seasonally distinctive climatic changes (e.g., Ljungqvist et al., 2019), as these are responding to different forcing mechanisms (e.g., Perșoiu et al., 2019). On multidecadal time scales, summer climate over Europe is influenced, mainly, by the Atlantic Multidecadal Oscillation

30
35
40



(AMO). The AMO is a climate mode of variability associated with periodical anomalies of sea surface temperatures (SSTs) in northern, extratropical latitudes. The positive phase is characterized by positive SST anomalies spanning the whole North Atlantic Ocean and is associated with above normal temperature over the central and eastern part of Europe, while the negative phase is characterized by negative SST anomalies over the North Atlantic Ocean and is associated with below normal temperatures over the central and eastern part of Europe. Over Europe the influence of the AMO is clearest during the summer (Sutton and Dong, 2012; Ioniță et al., 2012; 2017; O'Reilly et al., 2017).

In temperate climatic region, one of the most sensitive environmental archives are ice caves (Homlund et al., 2005, Kern and Perşoiu, 2013), i.e., rock-caves hosting perennial accumulations of ice. In such caves, ice is deposited as layers of frozen water, that carry with them the original stable isotope composition of precipitation that further reflects changes in air temperature and thus are important proxies of past temperature and moisture source variability (Perşoiu et al., 2011a, 2011b). In such caves, ice forms by the freezing on infiltrating water, the later accumulating during the rainy season, between early summer and late autumn (depending on site-specific conditions). The Carpathian Mountains host several ice caves (Brad et al., 2018) that preserve a large variety of geochemical information on past climate and environmental changes (Fórizs et al., 2004; Kern et al., 2004; Citterio et al., 2005; Perşoiu et al., 2017).

Here, we present the first reconstruction of summer climate variability and large scale circulation drivers during the last 1000 years based on the $\delta^{18}\text{O}$ and $\delta^2\text{H}$ values measured in Focul Viu Ice Cave (Western Carpathian Mountains, Romania). We argue that the stable isotope composition of cave ice is a proxy for summer air temperatures, and show that during the past millennium changes in these climatic parameter were mainly the result of external forcing induced by the variability of the AMO. Further, we show that summer temperatures in Eastern Europe were generally stable during the past 1000 years, the MWP-LIA differences being induced by high winter temperature variability.

2 Site information

Focul Viu Ice Cave (FV, 107 m long, ~30 m deep) is located in the Central Bihor Mountains, Romania (46.27° N; 22.68° E, 1165 m above sea level, Fig. 1a, Perşoiu and Onac, 2019). The cave has a simple morphology (Fig. 1b, 1c), with a small entrance that opens into the Great Hall (68 × 46 m), which in turn is followed by a narrow gallery, the Little Hall (20 × 5 m). The ceiling of the Great Hall opens to the surface (Fig. 1c), allowing for direct precipitation to reach the cave. Below the opening and covering the entire surface of the Great Hall, a layered ice block developed, with an estimated thickness of 20 m and minimum volume of 30,000 m³ (Orghidan et al., 1984; Brad et al., 2018). The descendent morphology of the cave and the presence of the two openings determine a specific air circulation (Perşoiu and Onac, 2019), with cold air inflow through the lower entrance and warm air outflow through the upper one in winter, and slow convective circulation within the cave (with no air mass exchange with the exterior) during summer. As a consequence of this circulation, the cave has a specific climate, with negative temperatures following the external ones between October and April, and stable ones at 0 °C between May and September, when ice melts and absorbs the heat transferred to the cave's atmosphere by conduction through the air and rock.

A direct consequence of the predominantly negative air temperatures in the cave is the genesis, accumulation and preservation of ice (Fig. 1b, 1c). During summer, infiltrating rainwater accumulates on top of the existing ice block and at the onset of negative temperatures in September it starts to freeze, forming a 1-20 cm thick layer of ice. Infiltration of water during warm periods in winter adds supplemental layers of ice on top of the ice block, however, at the onset of melting in April/May, this winter ice melts away. The result of these processes is a multiannual, layered, ice block, consisting of annual couplets of clear ice (on top) and sediment reach debris ones (at the bottom). Inflow of warm water in wet summers could result in the rapid ablation of the ice at the top of the ice block, thus partly altering the annual layering of the ice block. The



processes behind cave ice formation by water freezing and the registration of environmental signals by various proxies (stable isotope composition of ice, pollen content etc) have been described from the nearby Scărișoara Ice Cave (Perșoiu and Pazdur, 2011; Feurdean et al., 2011) and, given the close similarities between the two caves, are pertinent for Focul Viu Ice Cave, as well. The one notable difference is the timing of onset of freezing: in Scărișoara Ice Cave, the onset of freezing is
5 delayed until late-autumn and early winter (Perșoiu et al., 2017), whereas in Focul Viu Ice Cave it starts in early autumn.

3 Methods

3.1 Drilling and stable isotope analyses

The FV ice core (4.87 m long, 10 cm diameter) was drilled in May 2016 from the Great Hall of FV Ice Cave (Fig. 1d) using a modified PICO electric drill (Koci and Kuivine, 1984) manufactured by Heavy Duties S.R.L., Cluj Napoca, Romania. The
10 ice core was cut in 1 cm thin layers (considering also the annual layering) in the cold room, except for the section between 290 and 320 cm below surface, where we intercepted a tree trunk. Each samples was sealed in plastic bags, allowed to melt at room temperature, transferred to 20 ml HDPE scintillation vials and stored at 4 °C prior to analysis.

Precipitation samples were collected monthly between March 2012 and December 2018 at Ghețar (GT, 46°29'28.45" N, 22°49'26.02" E, 1100 m asl, ~15 km SE of the location of FV Cave) using collectors built according to IAEA specification.

15 The sea surface temperature (SST) is extracted from the Extended Reconstructed Sea Surface Temperature data (ERSSTv5) (Huang et al., 2018). This dataset covers the period 1854 – present and has a spatial resolution of 2° x 2°. The AMO index used in this study has been obtained from https://climexp.knmi.nl/data/iamo_ersst_ts.dat and is based also on the ERSSTv5 data set.

Water samples were analyzed for stable isotope composition at the Stable Isotope Laboratory, Ștefan cel Mare University
20 (Suceava, Romania), using a Picarro L2130i CRDS analyzer connected to a high precision vaporizing module. All samples were filtered through 0.45 μm nylon membranes before analysis and manually injected into the vaporization module multiple times, until the standard deviation of the last four injections was less than 0.03 for δ¹⁸O and 0.3 for δ²H, respectively. The average of these last four injections was normalized on the SMOW-SLAP scale using two internal standards calibrated against VSMOW2 and SLAP2 standards provided by IAEA and used in our interpretation. A third standard was used to
25 check the long-term stability of the analyzer. The stable isotope composition of oxygen and hydrogen are reported using standard δ notation, with precision estimated to be better than 0.16 ‰ for δ¹⁸O and 0.7 ‰ for δ²H, respectively, based on repeated measurements of an internal standard.

3.2 Radiocarbon dating and age-depth model construction

The wide skylight above the Great Hall (Fig. 1c) allows for a large volume of organic matter to fall in the cave and be
30 subsequently trapped in the ice. During drilling, we have recovered over 40 samples of organic matter from large tree trunks to pieces of leaves. Only 14 were suitable for radiocarbon dating, out of which 2 were not datable due to extremely small sample mass. AMS radiocarbon analyses were performed at the Institute of Physics, Silesian University of Technology, Poland (Piotrowska, 2013). All of the samples were precleaned with standard acid-alkali-acid treatment, dried and subjected to graphite preparation using an AGE-3 system (by IonPlus, CH) equipped with a VarioMicroCube by Elementar elemental
35 analyzer and automated graphitization unit (Wacker et al., 2010; Nemeč et al., 2010). The ¹⁴C concentrations in graphite produced from unknown samples, Oxalic Acid II standards and coal blanks have been measured by the DirectAMS laboratory, Bothell, USA (Zoppi et al., 2007). The results are reported in Table 1. The radiocarbon dates have been subjected to calibration with the use of OxCal v4.3 (Bronk Ramsey, 2009) and IntCal13 calibration curve (Reimer et al., 2013) or NH1 curve (Hua et al., 2013) for one post-bomb date.



Because the organic material can fall into the cave decades to centuries before being trapped in ice (see Fig. 1b), we have carefully screened the radiocarbon results prior to age-depth modeling with the aim to select the most reliable dates forming a chronological sequence and not contradict the previously well-dated core reported by Maggi et al. (2008). In total, four dates were selected for age-depth modeling and a collection year AD 2014 was assigned for the top of the ice core. The model was constructed using the OxCal *P_Sequence* algorithm (Bronk Ramsey, 2008) with variable prior *k* parameter ($k=1$, U(-2,2); Bronk Ramsey and Lee, 2013) and extrapolated to the depth of 4.86 m. The agreement index of the model was 83.1 %, confirming good statistical performance when the threshold of 60 % is surpassed. The sections between dated depths were assumed to have a constant deposition rate. The complete age-depth model is shown in Fig. 2. For further analysis the mean age derived from the model was used, reported also in Table 1.

10 4 Results and discussions

4.1 Ice accumulation in Focul Viu Ice Cave

The results of the radiocarbon analyses performed on organic matter recovered from the ice are shown in Table 1, with the depth-age model shown in Fig. 2. The maximum age of the ice is 1026 cal BP at 4.45 m below surface (based on direct dating of organic remains) and 1099 cal BP at 4.86 m below surface (extrapolation). A rock embedded in the ice at 4.87 m below the surface stopped the drilling effort, but previous work in the cave has shown that the thickness of the ice block exceeds 15 m (Orghidan et al., 1984; Kern et al., 2004; Perşoiu and Onac, 2019).

The ice accumulation rate was 0.39-0.41 cm/year between AD 851 and 947, 0.29-0.37 cm/year between AD 952 and AD 1005, 0.36-0.38 cm/year between AD 1010 and AD 1215, 0.4-0.44 cm/year between AD 1220 and AD 1970, and 0.56 cm/years in the past 40 years, with an average of 0.42 cm/year for the entire ice core. The variability seen in the ice accumulation rate during the last 1000 years results from the variable processes involved in the growth and decay of cave ice. Ice can melt as a result of either warm summers with enhanced conductive heat transfer to the cave or wet summers, with rapid ablation resulting from water flowing on top of the ice block. Subsequently, ice growth is influenced by the amount of water existing at the onset of freezing, the timing of this onset (earlier or later in the year) and its duration. Thus, the resulting accumulation rate is a record of the complex interplay of these climatic conditions, being an indicator of both ice growth and melt. The relatively (compared to the ensuing periods) high accumulation rates registered between AD 810 and AD 1230 were likely the result of high amounts of water available in the cave, resulting from the generally wet conditions during the Medieval Warm Period (Feurdean et al., 2015; Perşoiu and Perşoiu, 2019). The period with the highest accumulation of ice occurred between AD 1230 and AD 1392, a period of enhanced Mediterranean moisture transport to the site and slightly warmer winters compared to the preceding and ensuing periods. We tentatively suggest that during this period, the enhanced autumn precipitations originating from the Mediterranean Sea, as evidenced by the high d -excess values in the Scărişoara Ice Cave record (Perşoiu et al., 2017) and the warm (and thus likely short) winters led to a deeper lake on top of the exiting ice block at the onset of the freezing period and thus to a high accumulation rate. After AD 1400, palaeoclimate records from the region indicate an abrupt increase in (summer) precipitation of Atlantic origin (Feurdean et al., 2015) and drop in winter temperature (Perşoiu et al., 2017) likely causing rapid and sustained summer melting and early onset of freezing, thus resulting in an abrupt reduction of net ice accumulation. After AD 1450, the climate in the region was dominated by dry (but with frequent storms) summers and cold winters (Perşoiu, 2017), conditions that translate in low amounts of water available for freezing in early autumn, no inflow of water and thus now winter ice accumulation and enhanced summer melting – translating in minimal ice accumulation rates.



4.2 Stable isotopes in Focul Viu cave ice - proxy for summer air temperatures and AMO variability

The variability of $\delta^{18}\text{O}$ (and $\delta^2\text{H}$) in precipitation at Ghețar (10 km south of the cave's location and at the same altitude), assessed for the 2012-2017 period, follows that in temperature (Fig. 3a), with the maximum values (-3.6 ‰ and -26 ‰, for $\delta^{18}\text{O}$ and $\delta^2\text{H}$, respectively) in July/August and the minimum ones (-19.8 ‰ and -140 ‰, for $\delta^{18}\text{O}$ and $\delta^2\text{H}$, respectively) in 5 January. Similar result have been found by Bojar et al. (2009) and Ersek et al. (2018) for the same region, suggesting that the $^{18}\text{O}/^{16}\text{O}$ (and $^2\text{H}/^1\text{H}$) ratios in precipitation registers temperature changes on a regional scale. The Local Meteoric Water Line, defined by the equation $\delta^{18}\text{O} = 7.4 * \delta^2\text{H} + 6.1$ (Fig. 3b), has a slope and intercept nearly similar with those of Ersek et al. (2018). Precipitation in the region is mainly delivered by weather systems carrying moisture from the Atlantic Ocean, with the Mediterranean Sea contributing moisture during autumn and winter (Nagavciuc et al, 2019). The deuterium excess (*d-excess* or *d*) in precipitation, defined as $d = \delta^2\text{H} - 8 * \delta^{18}\text{O}$ (Dansgaard, 1964) allows for a clear separation of the two types of 10 air masses; its values being close to the global average of 10 (Craig, 1961) for moisture sourced from the Atlantic Ocean, and between 12 and 17, for moisture sourced in the Mediterranean Sea (resulting from the high evaporative conditions in the Eastern Mediterranean Sea). Similarly high values of *d-excess* have been measured by Drăgușin et al. (2017) in precipitation in SW Romania and Bădăluță et al. (2019) in precipitation in NE Romania, and linked to air masses originating in the 15 strongly evaporated Mediterranean and Black seas, respectively.

The FV $\delta^{18}\text{O}_{\text{ice}}$ and $\delta^2\text{H}_{\text{ice}}$ records span the AD 850 – AD 2016 period, showing generally stable values throughout the analyzed period, on which decadal to multi-decadal scale oscillations are superimposed. Both records display a remarkable similarity throughout the entire period, and in our discussion we have used only $\delta^{18}\text{O}$.

Observations on the dynamics of cave ice during the past 18 years have shown that it starts to grow in early autumn by 20 the freezing of water accumulated during summer. As the ceiling of the cave is opened to the exterior, precipitation directly reaches the site of ice formation, so that the stable isotope composition of precipitation is not modified in the epikarst above the cave (Moldovan et al., 2012; Ersek et al., 2018), thus preserving the original $\delta^{18}\text{O}$ (and $\delta^2\text{H}$) values of summer (June-July-August, JJA) precipitation. Further, $\delta^{18}\text{O}$ and $\delta^2\text{H}$ values in the FV ice core from the past 20 years are similar to values registered in the summer (JJA) precipitation at Ghețar (Fig. 3b) further supporting our inference that stable isotope values in 25 cave ice preserve the summer climatic signal. However, while freezing processes in caves could alter the original $\delta^{18}\text{O}$ (and $\delta^2\text{H}$) values in cave ice, Perșoiu et al. (2011b) have shown, from the nearby Scărișoara Ice Cave, that the original climatic signal embedded in the stable isotope composition of cave ice is preserved and can be used as a proxy for external climate variability.

Overall, our observations of cave ice genesis and dynamics and stable isotope monitoring data clearly indicate that 30 summer air temperatures are registered and preserved in the ice block in FV Cave. In order to test the long-term preservation of these connections, we have analyzed the links between the FV $\delta^{18}\text{O}_{\text{ice}}$ record and instrumental data from three nearby meteorological stations over the AD 1851 – AD 2016 period. On multidecadal time scales, summer air temperature changes in the region are controlled mainly by the dynamics of the Atlantic Multidecadal Oscillation (Ionita et al., 2012). Fig. 4. shows the JJA air temperature at Baia Mare (BM), Sibiu (SB) and Timișoara (TM) stations, the AMO index and FV $\delta^{18}\text{O}_{\text{ice}}$. 35 The instrumental temperature data indicates large multidecadal variability, with a cold period between AD 1890 and AD 1920, followed by a warm period between AD 1921 and AD 1960, a slightly colder period between AD 1960 and AD 2000, and enhanced warming over the last two decades, all following the AMO variability. The $\delta^{18}\text{O}_{\text{ice}}$ values show a similar temporal evolution, the slight offsets between the observational data and $\delta^{18}\text{O}$ being likely due to the dating uncertainty (20 – 35 years). Since the variability of AMO index is strongly associated with the prevailing sea surface temperature (SST) 40 anomalies over the North Atlantic Ocean basin (Sutton and Dong, 2012), we have computed the correlation map between the summer mean air temperature at SB station (with the longest instrumental record) and the summer SST. To remove short term variability and retain only the multidecadal signal in our data, prior to the correlation analysis, both the temperature time



series and the SST data were smoothed with a 21-year running mean filter. Figure 5 clearly shows that positive (negative) temperature anomalies over the analyzed region are associated with positive (negative) SST anomalies over the North Atlantic Ocean, resembling the SST anomalies associated with the positive (negative) phase of AMO (Mesta-Núñez and Enfield 1999, Latif et al. 2004; Knight et al. 2005). These results are also in agreement with the results of Della-Marta et al. (2007), showing that extreme high temperatures over Europe are triggered, at least partially, by the phase of AMO. A recent study of $\delta^{18}\text{O}$ variability in oak tree rings in NW Romania (~50 km NW from our site) also indicates the influence of the AMO on summer temperatures and drought conditions (Nagavciuc et al., 2019a). A potential physical mechanisms for the multidecadal variability of $\delta^{18}\text{O}$ in our ice cave can be as follows: prolonged periods of positive temperature anomalies throughout the summer months, due to prolonged warm SST in the North Atlantic Ocean, lead to high values of $\delta^{18}\text{O}$ at our site location via enhanced ice melting, while prolonged cold summers, due to a cold North Atlantic Ocean, lead to more negative $\delta^{18}\text{O}$ values.

Combining all data above, it results that, on time scales ranging from years to decades, prolonged periods of positive temperature anomalies throughout the summer months, linked to prolonged warm SSTs in the North Atlantic Ocean (and thus a positive AMO index), could be preserved by the $\delta^{18}\text{O}_{\text{ice}}$ in FV Ice Cave. We have compared the FV $\delta^{18}\text{O}_{\text{ice}}$ with tree ring width (TRW) reconstruction of JJA temperature anomalies (Popa and Kern, 2009). The highest similarities between the FV ice core and TRW records were found for the cold periods between AD 1000 – 1050, 1250 – 1300, 1420 – 1680, 1750 – 1850 and 1960 – 1980 and the warm periods during AD 1080 – 1200, 1850 – 1960. In contrast, some differences have been identified during the period AD 1640 – 1740, when the TRW record indicated above-average summer temperatures while the $\delta^{18}\text{O}$ record shows low values which suggest below – average summer temperatures (Fig. 7). Given the very different nature of the two archives (trees versus cave ice), of the proxies (TRW and $\delta^{18}\text{O}$) and of the chronologies (annual tree ring counting vs. ^{14}C dating), the two records agree remarkably well, further supporting the hypothesis that $\delta^{18}\text{O}$ (and $\delta^2\text{H}$) values in FV ice core is registering both summer air temperature variability during the past ca. 1000 years in East-Central Europe, as well as, on a broader spatial scale, the variability of the AMO.

Similar to the AD 1850-2016 interval described above, the stable isotope record closely mirrors the AMO variability over the entire studied interval (Fig. 6), suggesting a possible link between summer temperatures in Eastern Europe and solar influence. The relationship between the FV $\delta^{18}\text{O}_{\text{ice}}$ and AMO records is strongest between ~AD 1750 and AD 2016 and between AD 1125 and AD 1525, with decadal-scale variability in the two records being synchronous within the dating uncertainty (i.e., less than 30 years lag).

The apparent ~50 yrs lag of the FV $\delta^{18}\text{O}_{\text{ice}}$ record behind the AMO between AD 1600 and AD 1775 could have resulted from 1) high (> 50 years) uncertainty between AD 1525 and AD 1750, as well as before AD 1125 (Fig. 7a); 2) uncertainties in the reconstruction of AMO indexes before the instrumental record. Kilbourne et al. (2013) have shown, by comparing different proxy records of the AMO, that there is no consensus yet on the history of Atlantic multidecadal variability. Despite the similarities during the instrumental period, all the records they used in their study are quite different during the pre-instrumental era, most likely due to a lack of available well-dated, high-resolution marine proxy temperature records; 3) a less-straightforward link between solar forcing and the AMO (Knudsen et al., 2014) during the LIA. However, we do see the apparent breakdown of the correlation between summer temperatures and AMO only for a short period between AD 1600 and 1750, and also around AD 1050, periods when our chronology has the highest uncertainties. Further, the overall succession of high and low $\delta^{18}\text{O}$ values mimics the changes seen in the AMO reconstruction, so that the discrepancies could be the result of these uncertainties. If so, the record presented here suggest that solar-induced changes in the North Atlantic are transferred, likely *via* atmospheric processes, towards the wider Northern Hemisphere, resulting in hemispheric-wide climatic responses to perturbations in the North Atlantic



Several periods of excursions towards low $\delta^{18}\text{O}$ values (suggesting low summer temperatures) dot the past 1100 years (Fig. 7), the most notable one being around AD 870-930, AD 1030-1080, AD 1245-1355, AD 1425-1490, AD 1505-1550, AD 1680-1720, AD 1820-1850 and AD 1855-1925. Significant maxima occurred between AD 940-1030, AD 1100-1240 and AD 1630-1670. All these minima and maxima, except for the one centered on AD 1840 coincide (Fig. 7) with the known solar minima and maxima of the past 1000 years (the Spörer Minimum between AD 1450 and AD 1550 is split in two in our record, by a brief interval of possibly high temperatures around AD 1500).

The FV $\delta^{18}\text{O}_{\text{ice}}$ record is in agreement with other summer temperature reconstructions (Moberg et al., 2005; Buntgen et al., 2011) at regional and hemispheric scale (Fig. 7). Further, regional summer temperature reconstructions (Popa and Kern, 2009; Seim et al., 2012; Drăgușin et al., 2014) show warm peaks around AD 1320, 1420, 1560, 1780 and cooling around AD 1260, 1450 and 1820, similar with reconstructions and models at global level (Neukom et al., 2019) and the FV temperature reconstruction (this study). Contrary to the summer season temperature reconstructions, a late-autumn through early winter season temperature reconstructions from the nearby Scărișoara Ice Cave (Perșoiu et al., 2017) shows that the MWP was rather warm and also wet (Feurdean et al., 2011), while the LIA was cold, and likely drier (but with more erratically distributed precipitation, Perșoiu and Perșoiu, 2019). Together, these data suggest a complex picture of climate variability in the wider Carpathian region, with much of the yearly temperature variability during the past 1000 years being attributed to the influence of winter conditions, summer temperatures being rather constant. On this long-term trend, brief “excursions” were likely the result of large-scale circulation influences, with solar variability induced changes being transferred locally by atmospheric processes.

5 Conclusions

The analysis of the oxygen and hydrogen stable isotope ratios along a ~5 m long ice core extracted from Focul Viu Ice Cave (NW Romania) provided an unprecedented view on the dynamics of summer air temperature and atmospheric circulation changes during the past 1000 years in the poorly investigated East-Central Europe. The data shows little millennial-scale summer temperature variability since the onset of the Medieval Warm Period and through the Little Ice Age. Well-expressed minima and maxima occurred synchronously with periods of low and high solar activity, possibly suggesting a causal mechanism. Similarly, decadal-scale summer temperature variability follows that of the Atlantic Multidecadal Oscillation, and we subsequently hypothesize that solar-induced changes in summer climatic conditions over the Northern Atlantic are transferred through atmospheric processes across the Northern Hemisphere. Similar records from further east are thus required to test this hypothesis. Contrary to summer temperatures, winter ones show stronger contrast between the MWP and LIA, thus suggesting that the later were likely an expression of winter climatic conditions.

30

Author contributions. CAB and AP designed the project, AP and CAB collected the ice core and CAB performed the stable isotope analyses. NP performed the radiocarbon analyses and constructed the depth-age model. MI analyzed the climate and large-scale circulation data. CBD and AP wrote the text, with input from MI and NP.

35 **Competing interests.** The authors declare that they have no conflict of interest.

Data availability. The Focul Viu $\delta^{18}\text{O}$ and $\delta^2\text{H}$, as well as the ^{14}C data and the modeled ages will be made available upon publication, both on the CP webpage and on the NOAA/World Data Service for Paleoclimatology webpage. The meteorological data plotted in figure 4 was provided by the Romanian National Meteorological Administration, except for



the AMO data (panel a) which was downloaded from https://climexp.knmi.nl/data/iamo_ersst_ts.dat. The paleoclimate data used to plot fig. 7, panels a, b, c, d, f and g was downloaded from the NOAA/World Data Service for Paleoclimatology webpage. Data used in fig. 7e was provided by Virgil Drăgușin and is published in Drăgușin et al. (2014).

Acknowledgments. The research leading to these results has received funding from EEA Financial Mechanism 2009- 2014 under the project contract no CLIMFOR18SEE. AP was partial financially supported by UEFISCDI Romania through grants no. PN-III-P1-1.1-TE-2016-2210 and PNII-RU-TE-2014-4-1993. MI was partially supported by the AWI Strategy Fund Project PaLEX and by the Polar Regions and Coasts in the Changing Earth System (PACES) program of the AWI. We thank the Administration of the Apuseni National Park for granting permission to drill in Focul Viu Ice Cave, Nicodim Pașca for collecting precipitation samples, dr. Christian Ciubotărescu for help during the ice core drilling effort and Vlad Murariu (Heavy Duties Romania) for developing and constructing the drilling equipment.

Financial support. The article processing charges for this open-access publication were covered by the project EXCALIBUR of the Stefan cel Mare University of Suceava, Romania.

15

20

25

30

35

40



References

- Bădăluță, C.-A., Perșoiu, A., Ionita, M., Nagavciuc, V., and Bistricean, P. I.: Stable H and O isotope-based investigation of moisture sources and their role in river and groundwater recharge in the NE Carpathian Mountains, East-Central Europe, *Isot. Environ. Healt. S.*, 55 (2), 161–178, <https://doi.org/10.1080/10256016.2019.1588895>, 2019.
- 5 Brad, T., Bădăluță C.-A., and Perșoiu, A.: Ice caves in Romania, in: *Ice caves*, edited by: Perșoiu, A. and Lauritzen, S.-E., Elsevier, Amsterdam, Netherlands, 511–528, <https://doi.org/10.1016/B978-0-12-811739-2.00025-5>, 2018.
- Bojar, A., Ottner, F., Bojar, H. P., Grigorescu, D., and Perșoiu, A.: Stable isotope and mineralogical investigations on clays from the Late Cretaceous sequences, Hațeg Basin, Romania, *Appl. Clay Sci.*, 45, 155–163, <https://doi.org/10.1016/j.clay.2009.04.005>, 2009.
- 10 Bronk Ramsey, C. and Lee, S.: Recent and Planned Developments of the Program OxCal, *Radiocarbon*, 55, 720–730, <https://doi.org/10.1017/S0033822200057878>, 2013.
- Bronk Ramsey, C.: Bayesian analysis of radiocarbon dates, *Radiocarbon*, 51, 337–360, 2009.
- Bronk Ramsey, C.: Deposition models for chronological records, *Quaternary Sci. Rev.*, 27, 42–60, <https://doi.org/10.1016/j.quascirev.2007.01.019>, 2008.
- 15 Büntgen, U., Tegel, W., Nicolussi, K., McCormick, M., Frank, D., Trouet, V., Kaplan, J. O., Herzig, F., Heussner, K.-U., Wanner, H., Luterbacher, J., and Esper, J.: 2500 Years of European Climate Variability and Human Susceptibility, *Science*, 331, 578–582, <https://doi.org/10.1126/science.1197175>, 2011.
- Citterio, M., Turri, S., Perșoiu, A., Bini, A., and Maggi, V.: Radiocarbon ages from two ice caves in the Italian Alps and the Romanian Carpathians and their significance, In: *Glacier Caves and Glacial Karst in High Mountains and Polar Regions*, edited by: Mavlyudov, B. R., Institute of geography of the Russian Academy of Sciences, Moscow, Russia, 87–92, 2005.
- 20 Coumou, D., and Rahmstorf, S.: A decade of weather extremes, *Nat. Clim. Change*, 2, 491–496, <https://doi.org/10.1038/nclimate1452>, 2012.
- Craig, H.: Isotopic variations in meteoric waters, *Science*, 133, 1702–1703, <https://doi.org/10.1126/science.133.3465.1702>, 1961.
- 25 D'Arrigo, R., Wilson, R., and Jacoby G.: On the long-term context for late twentieth century warming, *J. Geophys. Res.*, 111, D03103, <https://doi.org/10.1029/2005JD006352>, 2006.
- Dansgaard, W.: Stable isotope in precipitation, *Tellus*, 16, 436–438, <https://doi.org/10.1111/j.2153-3490.1964.tb00181.x>, 1964.
- 30 Della-Marta, P. M., Luterbacher, J., von Weissenfluh, H., Xoplaki, E., Brunet, M., and Wanner, H.: Summer heat waves over western Europe 1880–2003, their relationship to large scale forcings and predictability, *Clim. Dynam.*, 29, 251–275, <https://doi.org/10.1007/s00382-007-0233-1>, 2007.
- Drăgușin, V., Staubwasser, M., Hoffmann, D. L., Ersek, V., Onac, B. P., and Vereș, D.: Constraining Holocene hydrological changes in the Carpathian-Balkan region using speleothem $\delta^{18}\text{O}$ and pollen based temperature reconstructions, *Clim. Past.*, 10, 1363–1380, <https://doi.org/10.5194/cp-10-1363-2014>, 2014.
- 35 Drăgușin, V., Bălan, S., Blamart, D., Forray, F. L., Marin, C., Mirea, I., Nagavciuc, V., Perșoiu, A., Tîrlă, L., Tudorache, A., and Vlaicu, M.: Transfer of environmental signals from surface to the underground at Ascunsă Cave, Romania, *Hydrol. Earth Syst. Sci.*, 21, 5357–5373, <https://doi.org/10.5194/hess-21-5357-2017>, 2017.
- 40 Ersek, V., Onac, B. P., and Perșoiu, A.: Kinetic processes and stable isotopes in cave dripwaters as indicators of winter severity, *Hydrol. Process.*, 32, 2856–2862, <https://doi.org/10.1002/hyp.13231>, 2018.



- Feurdean, A., Perşoiu, A., Pazdur, A., and Onac, B. P.: Evaluating the palaeoecological potential of pollen recovered from ice in caves: a case study from Scarisoara Ice Cave, Romania, *Rev. Palaeobot. Palyno.*, 165, 1–10, <https://doi.org/10.1016/j.revpalbo.2011.01.007>, 2011.
- 5 Feurdean, A., Galka, M., Kuske, E., Tanfău, I., Lamentowicz, M., Florescu, G., Liakka, J., Hutchinson, S. M., Mulch, A., and Hickler, T.: Last Millennium hydro-climate variability in Central Eastern Europe (Northern Carpathians, Romania), *Holocene*, 25, 1179–1192, <https://doi.org/10.1177/0959683615580197>, 2015.
- Fórizs, I., Kern, Z., Szántó, Zs., Nagy, B., Palcsu, L., Molnár, M.: Environmental isotopes study on perennial ice in the Focul Viu Ice Cave, Bihor Mountains, Romania. *Theor. App. Karst.*, 17, 61–69, 2004.
- Haustein, K., Allen, M. R., Forster, P. M., Otto, F. E. L., Mitchell, D. M., Matthews, H. D., and Frame, D. J.: A real-time
10 Global Warming Index, *Sci. Rep.*, 7: 15417, <https://doi.org/10.1038/s41598-017-14828-5>, 2017.
- Holmlund, P., Onac, B. P., Hansson, M., Holmgren, K., Morth, M., Nyman, M., and Perşoiu, A.: Assessing the palaeoclimate potential of cave glaciers: the example of the Scărişoara Ice Cave (Romania), *Geogr. Ann. A*, 87A, 193–201, <https://doi.org/10.1111/j.0435-3676.2005.00252.x>, 2005.
- Hua, Q., Barbetti, M., and Rakowski, A. Z.: Atmospheric Radiocarbon for the Period 1950–2010, *Radiocarbon*, 55, 2059–
15 2072, https://doi.org/10.2458/azu_js_rc.v55i2.1, 2013.
- Huang, B., Angel, W., Boyer, T., Cheng, L., Chepurin, G., Freeman, E., Liu, C., and Zhang, H.-M.: Evaluating SST analyses with independent ocean profile observations, *J. Climate*, 31, 5015–5030, <https://doi.org/10.1175/JCLI-D-17-0824.1>, 2018.
- IPCC: Global warming of 1.5°C. An IPCC Special Report. Geneva, Switzerland,
20 <https://doi.org/10.1017/CBO9781107415324>, 2018.
- Ionita, M., Rimbu, N., Chelcea, S., and Patrut, S.: Multidecadal variability of summer temperature over Romania and its relation with Atlantic Multidecadal Oscillation, *Theor. Appl. Climatol.*, 113, 305–315, <https://doi.org/10.1007/s00704-012-0786-8>, 2012.
- Jones, P. D., Osborn, T. J., and Briffa, K. R.: The evolution of climate over the last millennium, *Science*, 292(5517), 662–
25 667, <https://doi.org/10.1126/science.1059126>, 2001.
- Jones, P. D., and Mann, M. E.: Climate over the past millennia, *Rev. Geophys.*, 42, RG2002, <https://doi.org/10.1029/2003RG000143>, 2004.
- Jones, P. D., Briffa, K. R., Osborn, T. J., Lough, J. M., van Ommen, T. D., Vinther, B. M., Luterbacher, J., Wahl, E. R.,
30 Zwiers, F. W., Mann, M. E., Schmidt, G. A., Ammann, C. M., Buckley, B. M., Cobb, K. M., Esper, J., Goosse, H., Graham, N., Jansen, E., Kiefer, T., Kull, C., Küttel, M., Mosley-Thompson, E., Overpeck, J. T., Riedwyl, N., Schulz, M., Tudhope, A. W., Villalba, R., Wanner, H., Wolff, E., and Xoplaki, E.: High-resolution palaeoclimatology of the last millennium: A review of current status and future prospects, *The Holocene*, 19, 3–49, <https://doi.org/10.1177/0959683608098952>, 2009.
- Kern, Z., and Perşoiu, A.: Cave ice - the imminent loss of untapped mid-latitude cryospheric palaeoenvironmental archives,
35 *Quaternary Sci. Rev.*, 67, 1-7, <https://doi.org/10.1016/j.quascirev.2013.01.008>, 2013.
- Kern, Z., Fórizs, I., Nagy, B., Kázmér, M., Gál, A., Szántó, Z., Palcsu, L., and Molnár, M.: Late Holocene environmental changes recorded at Gheţarul de la Focul Viu, Bihor Mountains, Romania, *Theor. App. Karst.*, 17, 51–60, 2004.
- Kilbourne, K. H., Alexander, M. A., and Nye, J. A.: A low latitude paleoclimate perspective on Atlantic multidecadal variability, *J. Marine Syst.*, 133, 4–13, <https://doi.org/10.1016/j.jmarsys.2013.09.004>, 2013.
- 40 Knight, J. R., Allan, R. J., Folland, C. K., Vellinga, M., and Mann, M.E.: A signature of persistent natural thermohaline circulation cycles in observed climate, *Geophys. Res. Lett.*, 32, L20708, <https://doi.org/10.1029/2005GL024233>, 2005.



- Knudsen, M. F., Jacobsen B. H., Seidenkrantz, M.-S., and Olsen, J.: Evidence for external forcing of the Atlantic Multidecadal Oscillation since termination of the Little Ice Age, *Nat. Commun.*, 5: 3323, <https://doi.org/10.1038/ncomms4323>, 2014.
- Koci, B. R., and Kuivinen, K. C.: The PICO lightweight coring auger, *J. Glaciol.*, 30, 244–245, <https://doi.org/10.3189/S0022143000006018>, 1984.
- Latif, M., Botset, E. R. M., Esch, M., Haak, H., Hagemann, S., Jungclaus, J., Legutke, S., Marsland, S., and Mikolajewicz, U.: Reconstructing, monitoring and predicting multidecadal-scale changes in the North Atlantic thermohaline circulation with sea surface temperature, *J. Climate*, 17, 1605–1614, [https://doi.org/10.1175/1520-0442\(2004\)017<1605:RMAPMC>2.0.CO;2](https://doi.org/10.1175/1520-0442(2004)017<1605:RMAPMC>2.0.CO;2), 2004.
- Ljungqvist, F. C., Seim, A., Krusic, P. J., González-Rouco, J. F., Werner, J. P., Cook, E. R., Zorita, E., Luterbacher, J., Xoplaki, E., Destouni, G., García-Bustamante, E., Aguilar, C. A. M., Seftigen, K., Wang, J., Gagen, M. H., Esper, J., Solomina, O., Fleitmann, D., and Büntgen, U.: European warm-season temperature and hydroclimate since 850 CE, *Environ. Res. Lett.*, 14, 084015, <https://doi.org/10.1088/1748-9326/ab2c7e>, 2019.
- Maggi, V., Turri, S., Bini, A., and Udisti, R.: 2500 Years of history in Focul Viu Ice Cave, Romania, In: Proceedings of the 3rd International Workshop on Ice Caves, edited by: Kadebskaya, O., Mavlyudov, B., and Patunin, M., Kungur Ice Cave, Russia, 11–15, 2008.
- Mann, M. E., Zhang, Z., Rutherford, S., Bradley, R., Hughes, M. K., Shindell, D., Ammann, C., Faluvegi, G., and Ni, F.: Global signatures and dynamical origins of the Little Ice Age and Medieval Climate Anomaly, *Science*, 326, 1256–1260, <https://doi.org/10.1126/science.117730>, 2009.
- Mesta-Núñez, A. M., and Enfield, D. B.: Rotated global modes of non-ENSO sea surface temperature variability, *J. Climate*, 12, 2734–2746, [https://doi.org/10.1175/1520-0442\(1999\)012<2734:RGMONE>2.0.CO;2](https://doi.org/10.1175/1520-0442(1999)012<2734:RGMONE>2.0.CO;2), 1999.
- Moberg, A., Sonechkin, D. M., Holmgren, K., Datsenko, N. M. and Karlén, W.: Highly variable Northern Hemisphere temperatures reconstructed from low- and high-resolution proxy data, *Nature*, 433, 613–617, <https://doi.org/10.1038/nature03265>, 2005.
- Moldovan, O., Meleg, I., and Perşoiu, A.: Habitat fragmentation and its effects on groundwater populations, *Ecology*, 5, 445–452, <https://doi.org/10.1002/eco.237>, 2012.
- Nagavciuc V., Bădăluță C.-A., Ionita M.: Tracing the Relationship between Precipitation and River Water in the Northern Carpathians Base on the Evaluation of Water Isotope Data, *Geosciences*, 9, 198; <https://doi.org/10.3390/geosciences9050198>, 2019.
- Nagavciuc, V., Ionita, M., Persoiu, A., Popa, I., Loader, N. J., and McCarroll, D.: Stable oxygen isotopes in Romanian oak tree rings record summer droughts and associated large-scale circulation patterns over Europe, *Clim. Dynam.*, 52, 6557–6568, <https://doi.org/10.1007/s00382-018-4530-7>, 2019a.
- Nemec, M., Wacker, L., and Gäggeler, H. W.: Optimization of the Graphitization Process at AGE-1, *Radiocarbon*, 52, 1380–1393, 2010.
- Neukom, R., Steiger, N., Gómez-Navarro, J.J., Wang, J. and Werner, J. P.: No evidence for globally coherent warm and cold periods over the preindustrial Common Era, *Nature*, 571, 550–554, <https://doi.org/10.1038/s41586-019-1401-2>, 2019.
- Orghidan, T., Negrea, Ş., Racoviţă, G., and Lascu, C.: Peşteri din România: ghid turistic. Ed. Sport-Turism, Bucureşti, 1984.
- O'Reilly, C. H., Woollings, T., and Zanna, L.: The Dynamical Influence of the Atlantic Multidecadal Oscillation on Continental Climate, *J. Climate*, 30, 7213–7230, <https://doi.org/10.1175/JCLI-D-16-0345.1>, 2017.
- PAGES 2K Consortium: Consistent multidecadal variability in global temperature reconstructions and simulations over the Common Era, *Nat. Geosci.*, 12, 643–649, <https://doi.org/10.1038/s41561-019-0400-0>, 2019.



- Perşoiu, A., and Pazdur, A.: Ice genesis and its long-term dynamics in Scărișoara Ice Cave, Romania, *The Cryosphere*, 5, 45–53, <https://doi.org/10.5194/tc-5-45-2011>, 2011.
- Perşoiu, A., Onac, B. P., and Perşoiu, I.: The interplay between air temperature and ice dynamics in Scărișoara Ice Cave, Romania. *Acta Carsologica*, 40, 445–456, <https://doi.org/10.3986/ac.v40i3.4>, 2011a.
- 5 Perşoiu, A., Onac, B. P., Wynn, J. G., Bojar, A.-V., and Holmgren, K.: Stable isotope behavior during cave ice formation by water freezing in Scărișoara Ice Cave, Romania, *J. Geophys. Res.*, 116, D02111, <https://doi.org/10.1029/2010JD014477>, 2011b.
- Perşoiu, A., Onac, B. P., Wynn, J. G., Blaauw, M., Ionita, M., and Hansson, M.: Holocene winter climate variability in Central and Eastern Europe, *Sci. Rep.*, 7: 1196, <https://doi.org/10.1038/s41598-017-01397-w>, 2017.
- 10 Perşoiu, A.: Climate evolution during the Late Glacial and the Holocene. In: *Landform dynamics and evolution in Romania*, edited by: Rădoane, M., and Vespremeanu-Stroe, A., Springer, Berlin, Heidelberg, Germany, 57–66. https://doi.org/10.1007/978-3-319-32589-7_3, 2017.
- Perşoiu, A., Ionita, M., and Weiss H.: Atmospheric blocking induced by the strengthened Siberian High led to drying in the Middle East during the 4.2 ka event – a hypothesis, *Clim. Past*, 15, 781–793, <https://doi.org/10.5194/cp-2018-161>, 2019.
- 15 Perşoiu, I., and Perşoiu, A.: Flood events in Transylvania during the Medieval Warm Period and the Little Ice Age, *Holocene*, 29, 85–96, <https://doi.org/10.1177/0959683618804632>, 2019.
- Perşoiu, A., and Onac, B. P.: Ice caves in Romania, In: *Cave and Karst Systems of Romania*, edited by: Ponta, G. M. L., and Onac, B. P., Springer, Berlin, Heidelberg, Germany, 455–465, https://doi.org/10.1007/978-3-319-90747-5_52, 2019.
- Piotrowska, N.: Status report of AMS sample preparation laboratory at GADAM Centre, Gliwice, Poland, *Nuclear Instruments and Methods in Physics Research Section B*, 294, 176–181, 2013.
- 20 Popa, I., and Kern, Z.: Long-Term Summer Temperature Reconstruction Inferred from Tree-ring Records from the Eastern Carpathians, *Clim. Dyn.*, 32, 1107–1117, <https://doi.org/10.1007/s00382-008-0439-x>, 2009.
- Reimer, P. J., Bard, E., Bayliss, A., Beck, J. W., Blackwell, P. G., Bronk Ramsey, C., Grootes, P. M., Guilderson, T. P., Hafliðason, H., Hajdas, I., Hatte, C., Heaton, T. J., Hoffmann, D. L., Hogg, A. G., Hughen, K. A., Kaiser, K. F.,
25 Kromer, B., Manning, S. W., Niu, M., Reimer, R. W., Richards, D. A., Scott, E. M., Southon, J. R., Staff, R. A., Turney, C. S. M., and van der Plicht J.: IntCal13 and Marine13 Radiocarbon Age Calibration Curves 0–50,000 Years cal BP, *Radiocarbon*, 55, 1869–1887, https://doi.org/10.2458/azu_js_rc.55.16947, 2013.
- Seim, A., Büntgen, U., Fonti, P., Haska, H., Herzig, F., Tegel, W., Trouet, V., and Treydte, K.: Climate sensitivity of a millennium-long pine chronology from Albania, *Clim. Res.*, 51, 217–228, <https://doi.org/10.3354/cr01076>, 2012.
- 30 Steinhilber, F., Beer, J., and Fröhlich, C.: Total solar irradiance during the Holocene, *Geophys. Res. Lett.*, 36, L19704, <https://doi.org/10.1029/2009GL040142>, 2009.
- Sutton, R. T., and Dong, B.: Atlantic Ocean influence on a shift in European climate in the 1990s, *Nat. Geosci.*, 5, 788–792, <https://doi.org/10.1038/ngeo1595>, 2012.
- Wacker, L., Nemeč, M., and Bourquin, J.: A revolutionary graphitisation system: Fully automated, compact and simple,
35 *Nucl. Instrum. Meth. B*, 268 (7–8), 931–934, 2010.
- Wang, J., Yang, B., Ljungqvist, F. C., Luterbacher, J., Osborn, T. J., Briffa, K. R., and Zorita, E.: Internal and external forcing of multidecadal Atlantic climate variability over the past 1,200 years, *Nat. Geosci.*, 10, 512–517, <https://doi.org/10.1038/ngeo2962>, 2017.
- Zoppi, U., Crye, J., Song, Q., and Arjomand A.: Performance evaluation of the new AMS system at Accium BioSciences,
40 *Radiocarbon*, 49, 173–182, 2007.

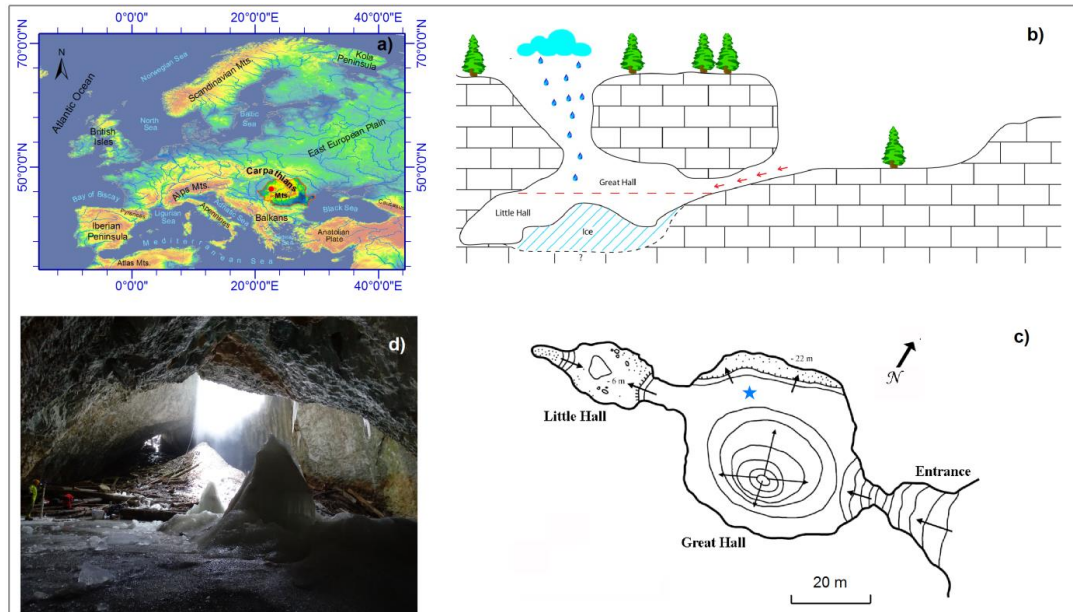


Figure 1. Location of the Focul Viu Ice Cave (red point) in Europe (a) and transversal (b) and longitudinal (c) cross section through the cave. The blue star (c) indicates the drilling point in the Great Hall (d) of the cave.

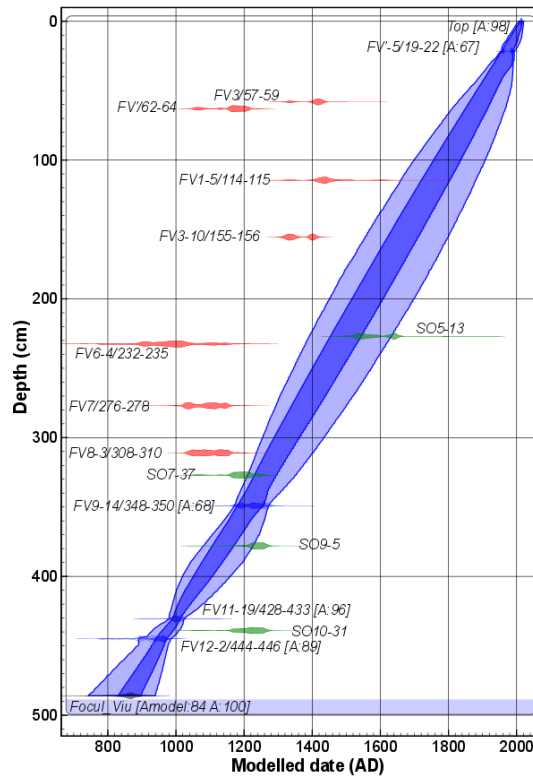


Figure 2. Depth age model of the Focul Viu ice core. The calibrated age range of dated samples is indicated in blue and the dates rejected in red. Green - dates from Maggi et al. (2008).

5

10

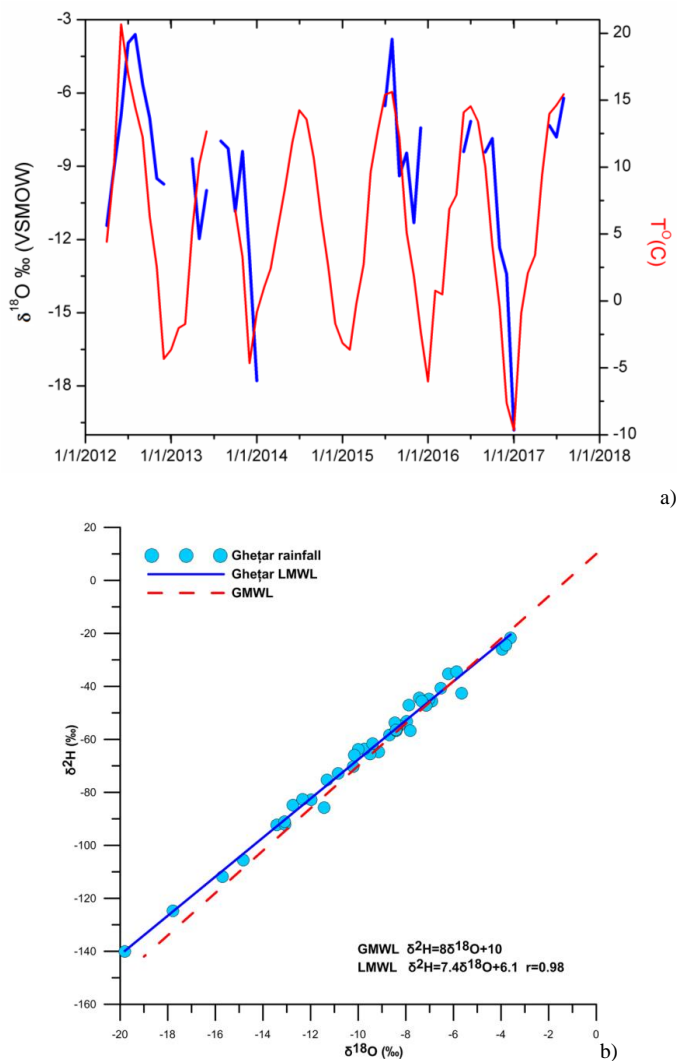


Figure 3. Temporal variability of $\delta^{18}\text{O}$ and $\delta^2\text{H}$ in precipitation and air temperature at Gheṭar and the LMWL for the same station, plotted against the GMWL.

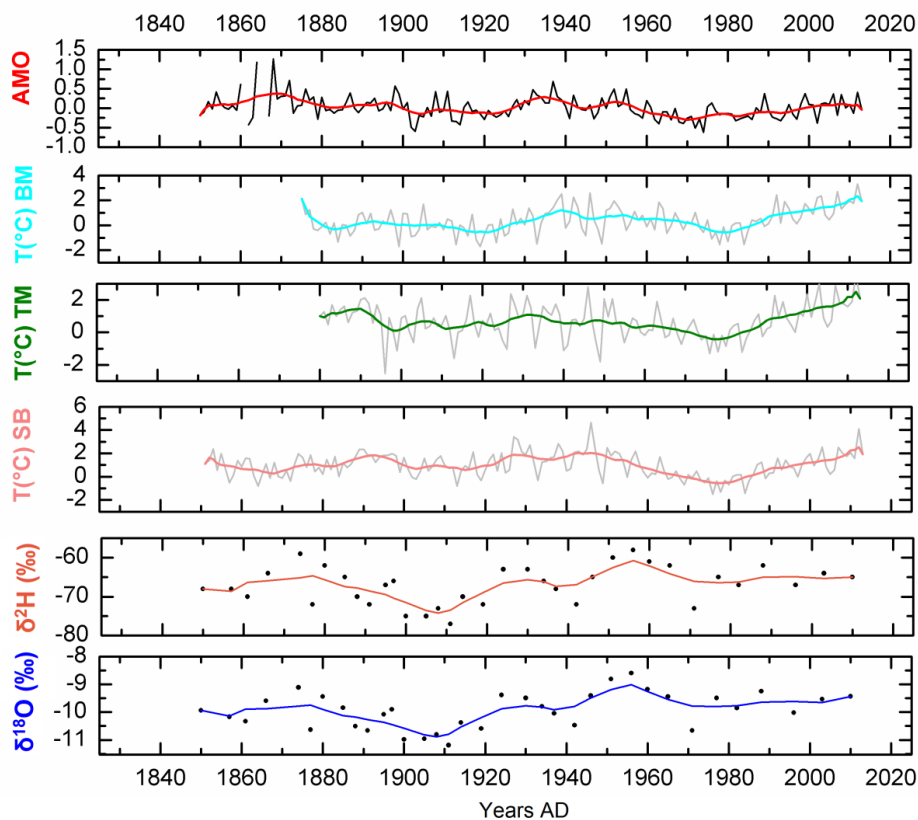


Figure 4. Temporal variability of the Atlantic Multidecadal Oscillation instrumental index, air temperature (anomalies with respect to the 1961-1990 period) recorded at Baia Mare (BM), Timișoara (TM) and Sibiu (SB) weather stations and FV $\delta^{18}\text{O}$ and $\delta^2\text{H}$ (‰) during the instrumental period. The thick lines represent 5 years moving averages for the $\delta^{18}\text{O}$ and $\delta^2\text{H}$ record, 5 and 11 years for the other records.



Sibiu TT JJA - SST JJA

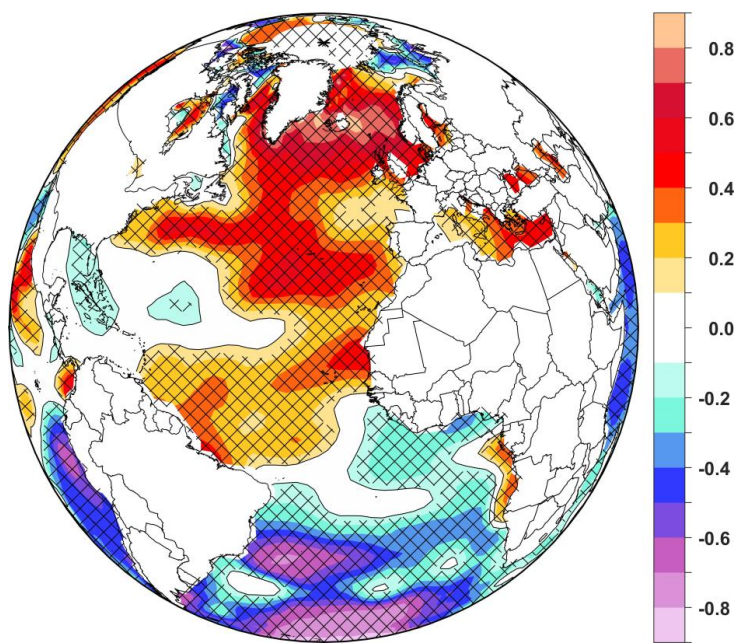


Figure 5. Spatial correlation map between SST and Sibiu Tmean in summer (JJA: June – July- August).
Analyzed period: 1850 - 2011

5

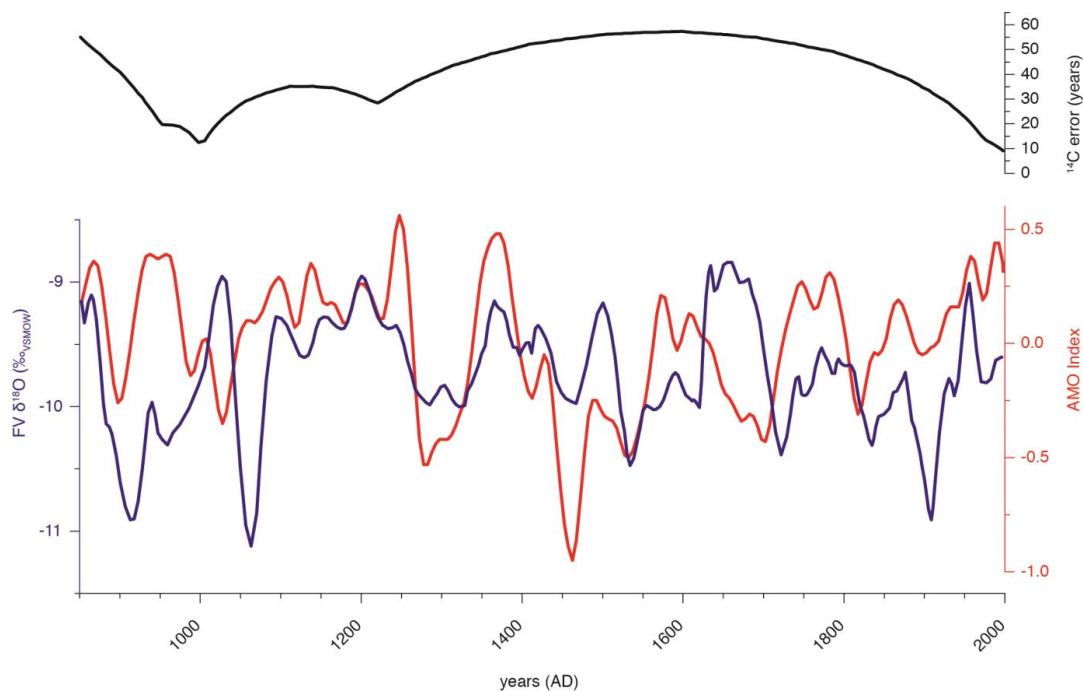


Figure 6. Temporal variability of the FV $\delta^{18}\text{O}$, reconstructed AMO index (Wang et al., 2017) and the ^{14}C measurement uncertainty.

5

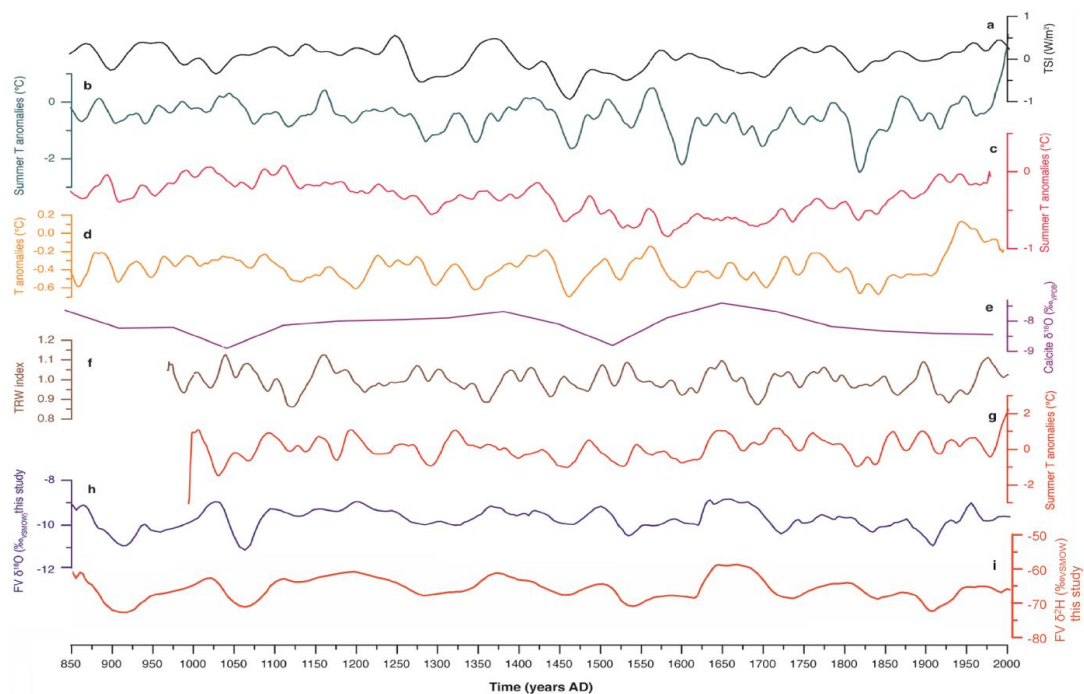


Figure 7. Summer climatic conditions recorded by $\delta^{18}\text{O}$ (and $\delta^2\text{H}$, panel i) from FV ice core (panel h, bottom) and comparison with proxy indicator from Nordic Hemisphere: a) Total Solar Radiation (Steinhilber et al., 2009), b) Central Europe summer temperature anomalies (against the 1901-2000 mean, Buntgen et al., 2011); c) Northern Hemisphere air temperature anomalies (against the 1961-1990 mean, Moberg et al. (2005); d) Northern Hemisphere air temperature anomalies (against the 1961-1990 mean, D'Arrigo et al., 2006), e) Speleothem $\delta^{18}\text{O}$ from SW Romania (Drăgușin et al., 2014); f) Tree Ring width index from Albania, SE Europe (Seim et al., 2012), g) Summer temperature anomalies in Romania (against the 1961-1990 mean, Popa and Kern, 2009).



Table 1. Radiocarbon data from the Focul Viu Ice Cave

No	Lab code GdA-	Sample name	Depth (cm)	Material	Sample mass (mgC)	¹⁴ C age (BP)	Status	Calibrated age range unmodelled (AD)	Modelled age mean age (AD)
1	4889	FV-5/19-22	21.5	needles and leaves, small fragments	0.86	-1410±25	accepted	1957-1992	1975±13
2	5084	FV3/57-59	58	leaf fragments	0.54	525±30	rejected	1322 1442	1891±36
3	4890	FV7/62-64	63	large wood fragment	1.00	875±25	rejected	1046 1223	1880±40
4	5085	FV15/114-115	114.5	needle fragment, small	0.25	470±50	rejected	1320-1619	1761±51
5	4891	FV3-10/155- 156	155.5	small wood fragment	0.61	570±25	rejected	1307-1420	1667±56
6	5086	FV6-4/232- 235	232.5	needles and leaves, small fragments	0.14	1045±70	rejected	778 1158	1489±56
7	4892	FV7/276-278	277	large wood fragment	0.99	960±35	rejected	1018 1158	1386±50
8	5087	FV8-3/308- 310	311	small plant fragments	0.90	925±25	rejected	1032 1162	1308±43
9	4893	FV9-14/348- 350	349	leaves, fragments	0.99	780±35	accepted	1190-1283	1220±30
10	5089	FV11-19/428- 433	430.5	small plant fragments	0.61	1030±20	accepted	984-1026	1001±12
11	5090	FV12-2/444- 446	445	small plant fragments	0.41	1140±20	accepted	777-977	953±20